

A STUDY ON A DIKE SWARM RELATED TO THE KÖNIGSPITZE (GRAN ZEBRU) PLUTON, ORTLER-CAMPO-CRYSTALLINE (VENOSTA VALLEY, W SOUTH TYROL): IMPLICATIONS ON MAGMA EVOLUTION AND ALTERATION PROCESSES

Volkmar Mair & Fridolin Purtscheller

With 7 figures and 3 tables

Abstract:

A dike swarm related to the Königspitze (Gran Zebrù) pluton of oligocene age intruded quartzphyllites and Triassic cover of the Ortler-Campo-Crystalline following pre-existent alpine structures. Two different types of intrusions are to be recognized: Type A are two phase intrusions like “sheeted dikes” following NNW-SSE fractures; Type B are andesitic dikes concordant to the EW striking schistosity of the quartzphyllites. Detailed field observation, petrographic work and mineral- and bulk rock chemistry show that these typical postcollisional intrusions are products of successive magma pulses originated from the same evolving magma chamber within a short time. The first magma pulse emplaced basalts, the second one andesites. Magma evolution through fractionation of amphibole, Al-poor clinopyroxene, magnetite and minor plagioclase is documented by the occurrence of cumulate xenoliths and xenocrysts of amphiboles and diopsides as well by major and trace element chemistry.

The dikes show different degrees of postmagmatic alteration, such as hydration of primary minerals and glassy matrix and changes in major and trace element chemistry due to fluid transport. The estimate of this secondary alteration allows the correct chemical classification even of the most altered samples using common classification diagrams developed for fresh, unaltered rocks.

Zusammenfassung:

Ein Schwarm von magmatischen Gängen im Gefolge des oligozänen Königspitz (Gran Zebru) Plutons intrudierte in die Quarzphyllite und triassischen Dolomite des Ortler-Campo-Kristallins. Die Intrusionen folgen vorgegebenen alpinen Stukturen und lassen sich in zwei Typen klassifizieren: Typ A sind zweiphasige Intrusionen in Form von „sheeted dikes“ welche in NNW-SSE-streichende saigere Klüfte intrudierten, Typ B sind andesitische Sills, konkordant zur EW-streichenden Schieferung des Quarzphyllits. Geländebelege, Petrographie, sowie Mineral- und Gesamtgesteinsschemie belegen, daß diese typischen postkollisionalen Gänge Produkte von schnell aufeinanderfolgenden Magmainjektionen einer evolvierenden Magmenkammer sind. Die erste Injektion lieferte Basalte, die zweite Andesite. Eine Magmenentwicklung durch Fraktionierung von Hornblende, Al-armen Clinopyroxen, Magnetit und wenig Plagioklas ist durch das Auftreten von Kumulatxenolithen, Xenokristallen von Hornblende und Diopsid, sowie durch die Haupt- und Spurenchemie belegt.

Die Intrusionen zeigen unterschiedlich starke postmagmatische Alteration, wie Hydratisierung des primären Mineralbestandes und der glasigen Matrix, sowie Änderungen in Haupt- und Spurenchemie durch Fluidtransport. Eine genaue Abschätzung dieser Alterationsprozesse erlaubt eine korrekte Klassifikation auch der stark alterierten Gesteinsproben mittels der üblichen Klassifikationsdiagramme, welche nur für frische Proben entwickelt wurden.

1. Introduction

Oligocene, postcollisional intrusions, emplaced along the Periadriatic suture, have been studied by several authors in attempt to reconstruct a geodynamic model of the Eastern Alps (GATTO et al., 1976; BECCALUVA et al., 1983; PURTSCHELLER & MOGESSIE, 1988; DAL PIAZ et al., 1989; and others). The various plutons, stocks and dikes are different in age and chemistry.

The typical orogenic character of calcalkaline/shoshonitic nature of these intrusions is well-documented, even if chronology and distribution of the magmatic bodies do not fit space and time versus composition relationships, which characterize most modern consuming plate margins. Geochemical and isotope data are documented for most of the large intrusions, but not for the numerous dike swarms. Beside that there is a great scatter of the chemical data since chemical differences do not only reflect the nature of the source region and magma generation but are strongly affected by later processes such as magmatic differentiation and/or accumulation. These processes are not known in detail even for the larger intrusions, except for the Adamello batholith and the Bergell intrusion (DAL PIAZ et al., 1979; LAUBSCHER, 1983; ULMER et al., 1983). In addition, there do not exist estimates of the influence of secondary alteration and weathering processes on these rocks.

2. Geological outlines

The intrusions of the Ortler-Campo-Crystalline were first described by STACHE & JOHN, 1879, as "suldenite" and "ortlerite". Most intrusive bodies are mapped on the Mt. Cevedale sheet (ANDREATTA, 1951). They are undeformed, cut the regional schistosity, the alpine folding and shear zones and intruded basement and Triassic covers. According to GATTO et al., 1976, they get older from SE (32 m.y.) towards NW (87 m.y.). While PURTSCHELLER & MOGESSIE,

1988, refer a chemical variation of the dikes from basaltic in the west (Ortler-Cevedale) to rhyolitic in the east (Hoher Dieb), DAL PIAZ et al., 1989, recognized two groups of magmatic bodies with calc-alkaline and high-K-calcalkaline/shoshonitic affinity in two adjacent and separate belts north and more or less parallel to the Pejo Line, which separates the overlapping Tonale Unit from the underlying Ortler Basement. The high-K-calcalkaline/shoshonitic group is represented by the Grünsee- and Mare Valley intrusive complexes and the Gavia Valley dikes. The calcalkaline group includes the Forno Valley andesitic dikes and the Gran Zebrù quartzdioritic pluton, discontinuously exposed in the glacier areas at the base of the southern wall of the Königspitze (Gran Zebrù), between the upper Zebrù Valley, the Pale Rosse and the Bottiglia Pass (fig. 1).

Fig. 2 shows the investigated dikes outcropping NE of the main intrusion, E of the Gran Zebrù between the upper Sulden- and Martell Valley. The dikes intruded the triassic dolomites and the quartzphyllite complex which is a sequence of metapelites with beds and lenses of marbles, quartzites and metabasites. Dikes crosscut schistosity and an eo-Alpine (THÖNI, 1983), north-verging shear zone, marked by carbonate-rich cataclasites, dolomite-, gypsum- and serpentinite lenses. Thermally overprinted xenoliths of the shear zone, together with those of the country rocks, forthcoming in most of the dikes.

Field observation shows that magma emplacement followed two different systems:

Type A: In the western region in the Triassic dolomites and in the quartzphyllites at the base of the dolomites the magma intruded in NNW-SSE striking, more or less vertical fractures. These 1.5 m to 4 m thick dikes are very interesting because they document a two-phase intrusion in form of a sheeted dike: the 50–70 cm thick outer parts consist of a dark „primitive“, the inner part of a light grey, more differentiated material. The boundaries between the basalt

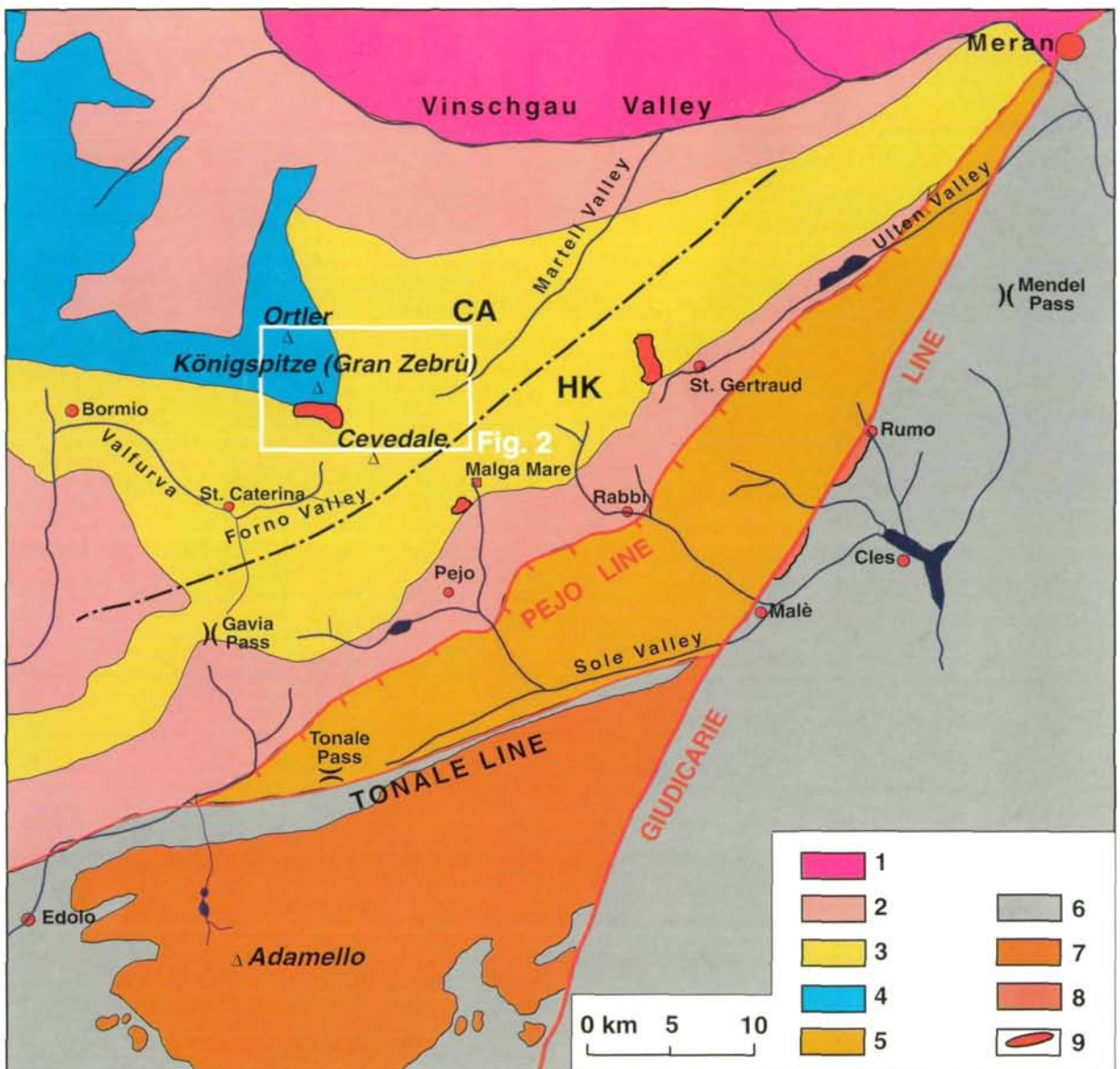


Fig. 1: Tectonic map showing the position of postcollisional intrusions.

The frame indicates the studied area; **Austroalpine units:** 1 Ötztal Stubai Altkristallin, 2 micaschists and paragneisses of Ortler nappe, 3 quartzphyllites and retrogressed paraschists, 4 sedimentary cover, 5 Tonale unit (high grade metamorphic); **Southern Alps:** 6 undifferentiated cover and basement sequences, 7 Adamello batholith; **Postcollisional intrusions:** 8 Rumo and Samoclevo lamellae, 9 major plutons, stocks and apophyses of calcalkaline (CA) and high-K calcalkaline/shoshonitic (HC) affinity (divided by stippled line). After DAL PIAZ et al., 1988.

rims and the younger andesite core are marked by chilled margins and fluidal structures due to mechanical mingling of the two phases (fig. 3a).

Type B: Intrusion of the dikes in the eastern part of the area followed the WSW–ENE striking

and 35° – 45° south-dipping schistosity and vertical WSW–ENE fractures of the quartzphyllites. Thus, the magmatic bodies seem to cover both, the aspect of sills, when following the schistosity, and of short dikes, where they follow the fractures (fig. 3b).

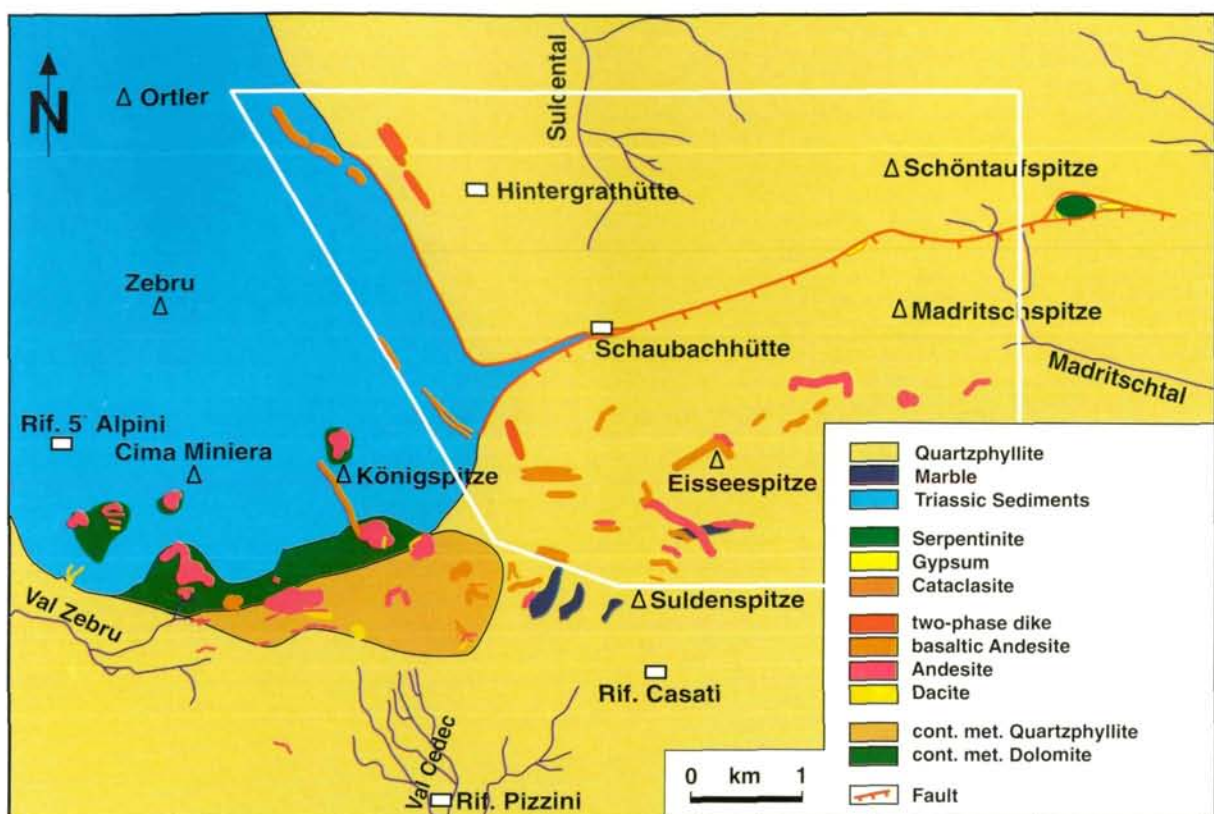


Fig. 2: Sketch map of the Königspitz (Gran Zebru) Pluton with related dikes. The frame indicates the investigated dikes.

3. Petrography and mineralogy

The thickness of the dikes varies from a few centimeters to 5 m, but only dikes thicker than 0.5 m are considered. The contacts to the country rocks are sharp and marked by chilled margins. Because of the small size of the dikes no sign of contact metamorphism is detected.

Based on field observation and detailed petrographic work, two rock types with different textures and mineral assemblages can be distinguished:

Type I is represented by the inner parts of the sheeted dikes and by a 1 m thick dike outcropping at the Eissee Pass. These dikes are very similar to those described by PURTSCHELLER & MOGESSIE, 1988. The paragenesis of these porphyric, black to dark-green basalts/basaltic andesites is characterised by large phenocrysts of

hornblende, clinopyroxene and plagioclase in a glassy matrix, sometimes containing minute plagioclase crystals. Magnetite and apatite are the most common accessories. Chlorite, calcite sericite and rare epidote are alteration products of this matrix. Calcite is not only dispersed in the groundmass but also occurs in small cavities.

The up to 2 cm long hornblendes are brown to green and occur as idiomorphic crystals and very often in agglomerates. All hornblendes display a slight oscillatory zoning. Some show a corroded rim but are rarely altered to calcite, chlorite, epidote and opaques.

Macroscopically the clinopyroxenes are not detectable. In thin sections they are unzoned, but often show a rim of amphiboles. No sign of alteration can be observed.

Plagioclase phenocrysts are rare and much smaller than the hornblendes and pyroxenes. Occurring as single crystals or as agglomerates some of them are optically unzoned, others are

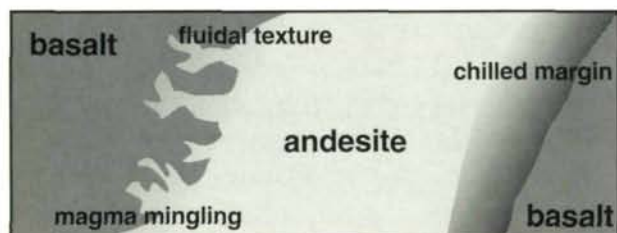
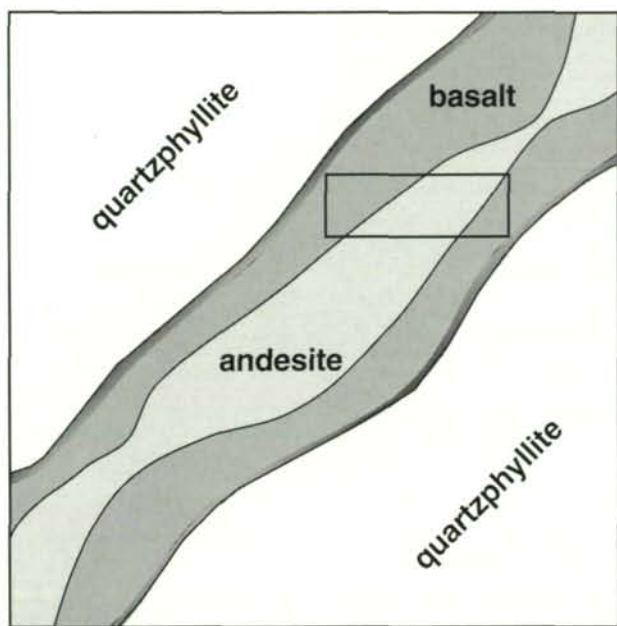


Fig. 3a

zoned. Very often the cores are altered to sericite and calcite. In the more altered samples the plagioclases are totally altered. Relictic anorthites are not visible, but sometimes the primary zonation of the plagioclase is preserved by zones of different sericitization.

The dikes bear rare xenoliths of country rocks with slight thermal overprint. Xenoliths of magmatic origin, such as cumulates, vesicles or other magmatic rocks are not detectable.

Type II represents the dikes of the eastern part and the outer parts of the two-phase intrusions. These dikes are the most frequent ones and very similar to those described by DAL PIAZ et al., 1989; they are considered to be products of the main intrusion phase.

The dikes are porphyritic with black, up to 5 cm long hornblende and white plagioclase-phenocrysts in a light grey glassy matrix with feldspar and magnetite. The alteration of the dif-

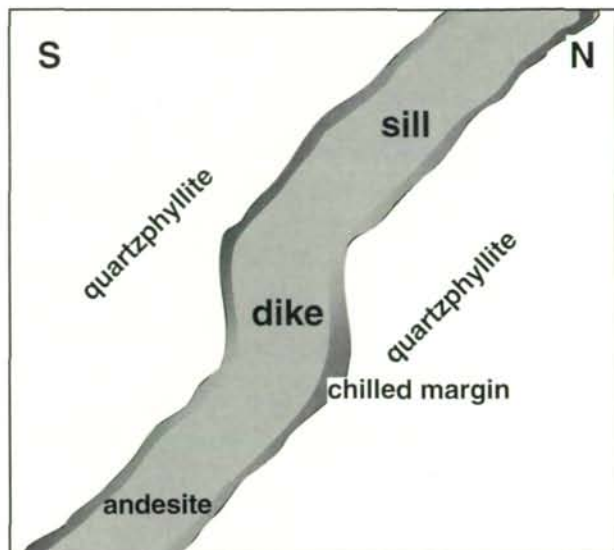


Fig. 3b

Fig. 3: Different intrusion mechanisms.

3a: Type A: two-phase intrusions; phase 1 (rim zone) basalt, phase 2 (inner zone) andesite.

3b: Type B: "common" intrusions of the eastern part of the area: concordant and discordant to the surrounding quartzphyllite.

ferent dikes varies from very fresh rocks where only the Ca-rich cores of the plagioclases are slightly sericitized, to samples where the phenocrysts and the whole matrix are altered to sericite, chlorite, calcite, minor epidote and opaques.

The plagioclase phenocrysts occur as single crystals, but more frequently as agglomerates of normal-zoned individual grains. While the larger crystals are idiomorphic, sometimes with corroded rims and sericitized cores, the smaller ones are totally sericitized.

The olive-green to brown-green hornblendes are always idiomorphic and show the same weak optical oscillatory zoning.

A second type of amphiboles occurs as accessory mineral. The crystals are idiomorphic but most of them have corroded rims. They show oscillatory zoning from a yellow-green core to a dark green rim. These amphiboles are xenocrysts of cumulitic origin.

Green pyroxenes with a diameter up to 2 cm are detectable in all dikes. They occur as idiomorphic, sometimes corroded grains and as relics in amphiboles and amphibole agglomerates.

All dikes bear contact-metamorphic xenoliths of the surrounding rocks and magmatic inclusions, cognate mafic nodules according to DAL PIAZ et al., 1989.

4. Magmatic inclusions

Magmatic inclusions with different textures and parageneses occur in all intrusions of Type B. Cognate inclusions are widespread but hardly visible in the field, as they show the same paragenesis as the dikes and differ only due to their fine-grained porphyritic texture. The contacts between inclusion and dike material are never sharp but show fluidal textures and rims of chemical/physical reactions between inclusion and dike material. The xenoliths display a chemistry between that of Type A and B dikes, sometimes with a higher amount of alkalis (see chapter bulk rock chemistry). They may be interpreted as fragments detached and brought up from the rim of the crystallizing magma chamber or as products from crystallization processes occurring within the host magma.

The most common inclusions (up to 15 cm in size) are rounded, coarse-grained hornblende-gabbros with cumulate texture. The contact to the dike material is marked by a rim of fine- to medium-grained amphiboles. The paragenesis of the cumulates is characterized by long-prismatic hornblendes + plagioclase + accessory magnetite ± clinopyroxene. The amphiboles are never altered, but the plagioclases sometimes show slight alteration to sericite and clinozoisite. The brown amphiboles are slightly zoned while the feldspars are unzoned. According to the bulk rock chemistry, these inclusions can be classified as nepheline-normative monzogabbros. Texture, paragenesis, chemistry and the elevated anorthite-content of the plagioclases strongly suggest that the hornblende gabbros originated from a basaltic melt by

fractional crystallization. The rounded to ellipsoidal forms of the inclusions may be caused by: an eruption of the magma chamber before a solid cumulate stratus developed, or convection in a stratified magma chamber due to repeated injection and migration of melts in and from the magma chamber (DAL PIAZ et al., 1979; LAUBSCHER, 1983; ULMER et al., 1983; CONRAD & KAY, 1984), or the formation of "drops" during the magma-ascent due to different viscosity of cumulates and melt (BACON, 1986).

5. Mineral Chemistry

Mineral compositions were analyzed using an ARL-SEMQ electron microprobe with four wavelength dispersive spectrometers and a NORAN energy dispersive system at the Institute of Mineralogy and Petrography, University of Innsbruck using standard conditions. Representative analyses are given in table 1.

Amphiboles

The brown-green amphiboles of the cumulates are unzoned or slightly zoned pargasites to magnesio-hastingsites (IMA classification, following LEAKE, 1978, and calculated with the computer program „EMP-AMPH“ of MOGESSIE, TESSADRI & VELTMAN, 1990). Where these cumulitic hornblendes occur as single xenocrysts in the dikes, they show weak optical and chemical zonation from magnesio-hastingsite in the core to ferri-tschermakitic hornblende in the rim, documenting a diminution of the edenite vector caused by uprising of the cumulitic inclusions.

The brown to green hornblendes of Type A and B are tschermakite to ferri-tschermakite in composition and display slight oscillatory zoning due to Fe(Mn)-Mg exchange, probably caused by cooling of the magma.

Clinopyroxenes

The pyroxenes occurring as relics in the cumulates and cumulitic xenocrysts of hornblende are almost pure, unzoned diopsides.

Macroscopically the pyroxenes of Type A are not detectable. In thin section they are unzonend and often have a rim of tschermakitic hornblende. Composition slightly varies from pure diopside to salite.

Type B pyroxenes occur with diameters up to 2 cm as idiomorphic, sometimes corroded grains and as relics in amphiboles and amphibole agglomerates. They are unzoned diopsides, comparable to those described by DAL PIAZ et al., 1989, from the Bottiglia Pass, and by ULMER et al., 1983 (Type 3, Monte Mattoni).

Feldspars

The feldspar of the cumulates is an almost pure, unzoned anorthite with An 95 to An 90, sometimes slightly altered to sericite.

In the dikes of Type A feldspar phenocrysts are much rarer than phenocrysts of hornblende or pyroxene. Only a few of the plagioclases are unzoned, most of them show optical and chemical zonation. Chemical profiles show a zonation from An 90 in the core to An 66 in the rim.

In the dikes of Type B feldspars occur as single crystals and, more frequent, as agglomerates of normal zoned individual grains. Chemical zonation ranges from bytownite (An 85) in the core to andesine (An 50) in the rim.

6. Bulk rock chemistry

Major elements have been analysed on fused rock samples with an ARL-SEMQ microprobe using standard conditions. Trace elements were measured with ICP-AES (Philips PU 7000) using LiBO₂-flux technique. Representative analyses are given in table 2.

Major elements

The two different rock types observed in the field differ from each other chemically. According to the TAS diagram (LE MAITRE, 1984; IUGS-Commission, 1988) (Fig. 4) Type A represents basalts /basaltic andesites with SiO₂ bet-

ween 51 wt% and 54 wt%; rocks of Type B are andesites with SiO₂ between 56.5 wt % and 60 wt %. A comparison with published data shows that Type A is similar to the Ortler basalts described by PURTSCHELLER & MOGESSIE, 1988 and Type B corresponds to the chemistry published by DAL PIAZ et al., 1988 for the Königspitz (Gran Zebru) Pluton. For comparative purposes representative analysis for cognate inclusions and a cumulate are plotted. While the hornblende gabbro cumulate falls into the picrite basalt field, the cognate inclusion displays a chemistry between that of Type A and Type B.

The Harker diagrams (fig. 5) imply that the two different phases are products of a continuous magma evolution. Increasing SiO₂ correlates with increasing alkalis and decreasing Fe₂O₃ (Fe tot), MgO and CaO. The AFM-diagram, the K₂O vs SiO₂ diagram after PECCERILLO and TAYLOR, 1976 and the TiO₂ vs FeO*/MgO diagram after MYASHIRO, 1973 show a typical calcalkaline differentiation trend. The TiO₂ values are below 1 wt% and decrease with increasing SiO₂. According to MYASHIRO, 1973; PEARCE & CANN, 1973 this is typical for calcalkaline rocks. The Al₂O₃ contents display a range from 16 wt% to 19 wt%. MnO, P₂O₅ and SO₃ do not show indicative trends.

Trace elements

While the compatible elements Co, Cr and V decrease with increasing SiO₂, the elements Ba, Rb and Sr are strongly enriched, with a great scatter in the andesites due to various degrees of alteration. The elements of the Ti-group, Zr, Nb and Y display low values, Zr is enriched, Nb decreases during magma evolution. According to GATTO et al., 1976; PECCERILLO et al., 1976; BECCALUVA et al., 1979; GILL, 1981; BECCALUVA et al., 1983 these trends of trace and major elements are typical of calcalkaline magmatism at convergent plate margins.

Magmatic differentiation trends based on trace element chemistry are consistent with the results of discrimination using major elements.

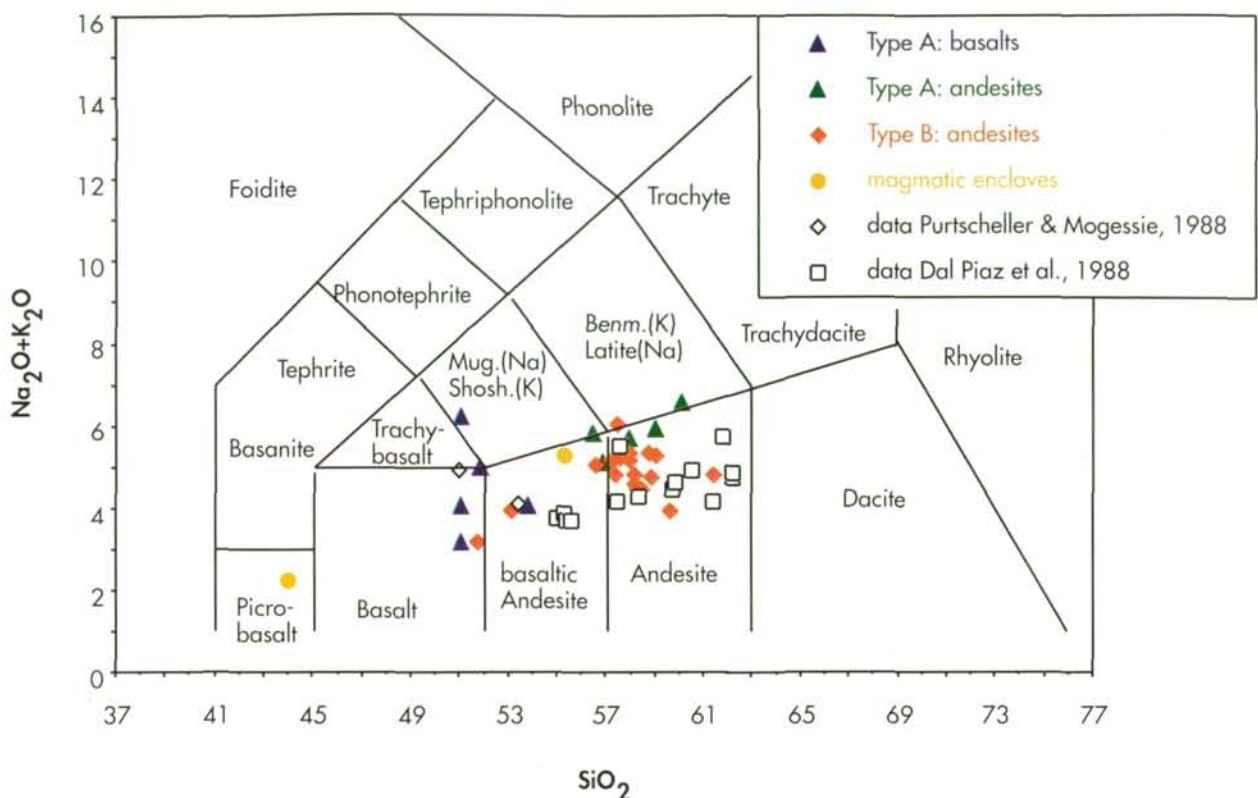


Fig. 4: The Total Alkali-Silica Diagram (LE BAS et al., 1992). The two intrusion phases are clearly separated. All dikes of the eastern part fall in the typical area for postcollisional magmatites of calc-alkaline series. Although there are different degrees of alteration, the scatter of the samples is quite low. For comparative purposes two magmatic inclusions and data from PURTSCHELLER & MOGESSIE, 1988, and DAL PIAZ et al., 1988, are plotted. All analyses recalculated to 100% loss-free.

7. Influence and degree of secondary alteration processes

Macroscopically most dikes appear very fresh, but slightly sericitized feldspars or chloritized amphiboles and loss on ignition (L.O.I.) values ranging from 1.8 wt% to 2.5 wt% indicate a slight secondary alteration of the rocks. L.O.I. values from 1 wt% to 7 wt% are reported for similar rocks by several authors (GATTO et al., 1976; BECCALUVA et al., 1983; DEUTSCH, 1984; VENTURELLI et al., 1984; DAL PIAZ et al., 1988; PURTSCHELLER & MOGESSIE, 1988); they are considered to be typical. A chemical classification of these dikes using the different discrimination diagrams is problematic, because the diagrams are developed exclusively for fresh rocks (e.g. the TAS-diagram is limited for rocks with L.O.I.-values < 2 wt%; LE BAS et al.,

1992). Therefore an estimate of various degrees of secondary alteration on petrography and chemistry of these dikes is needed!

An andesitic dike outcropping at the NW-ridge of the Eisseespitze, approximately in the center of the investigated area, turned out to be suitable for such an estimate. Crosscutting the quartzphyllites this approximately 3 m thick dike splits into two separate, parallel dikes, as shown in fig. 6. The main dike remains as thick as before the sharing, the second becomes thinner. After the distance of approximately 70 m it is only 30 cm thick. While the main dike suffered no alteration, the second shows increasing alteration with decreasing thickness. Therefore the alteration of the second dike is clearly caused by elevated penetration of postmagmatic fluids at one end of the dike and not by fluid infiltration of the whole area.

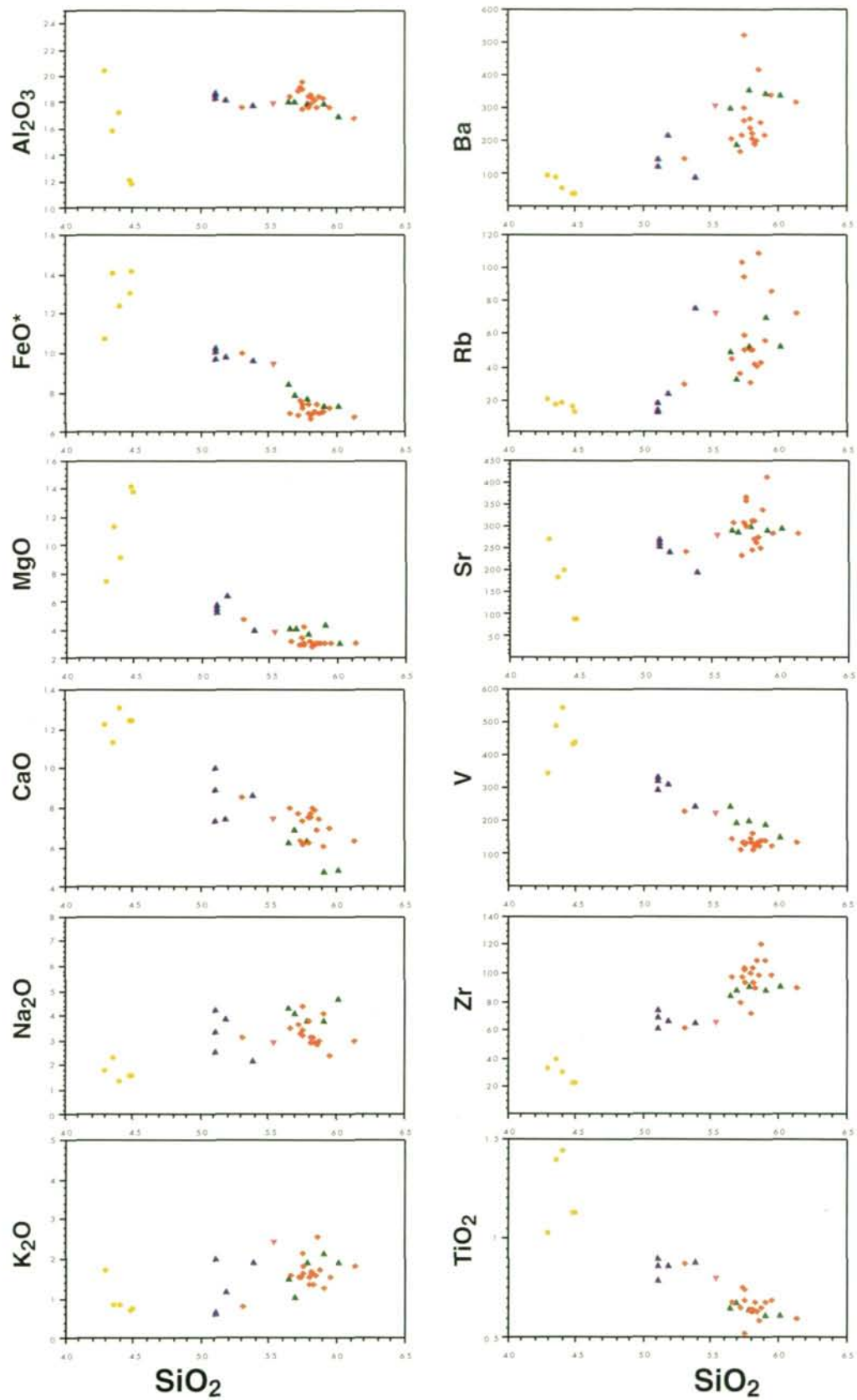


Fig. 5: Harker Diagrams for the most significant major and trace elements. For comparative purposes cumulates and a intermediate magmatic inclusion are plotted.

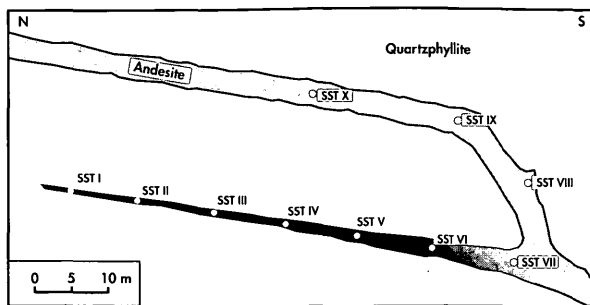


Fig. 6: The dike studied for the estimate of increasing secondary alteration with decreasing thickness. From the geometry of the dike it is clear, that the alteration processes are postmagmatic and related to the dike end and not to a regional fluid infiltration. Sample locations are indicated by their numbers.

Ten samples (SST I–SST X), collected every ten meters from the center of the dike (fig. 6), are analyzed for petrography, mineralogy, inclusions and chemistry. Changes in petrography and mineralogy of the respective samples, dependent on decreasing thickness (= increasing alteration), are listed in detail in table 3. Chemistry of the samples is determined after cutting them into 1 cm thick slices and removing the inclusions, that are analyzed separately.

The autohydrothermal fluids are rich in SO_4 and CO_2 . This is proved by the presence of cavities from 0.5 cm to 5 cm in diameter, filled with celestite and baryte and with calcite, laumontite and quartz. With increasing fluid flow the hornblende-phenocrysts are replaced by chlorite, epidote, calcite and pyrite, the feldspars by sericite and calcite. This replacement begins with chlorite growth along the cleavage of the amphiboles and the growth of sericite and laumontite in the Ca-rich feldspar cores, and ends with pseudomorph phenocrysts. The glassy matrix is increasingly replaced by chlorite, rare epidote and dispersed calcite and laumontite. Sometimes calcite and laumontite occur in form of agglomerates and in small cavities dispersed in the matrix.

The major elements do not show indicative trends.

The trace elements show different behavior (fig. 7): The mobile elements Sr and especially Ba and Rb are continuously enriched until being elevated enough to crystallize in specific

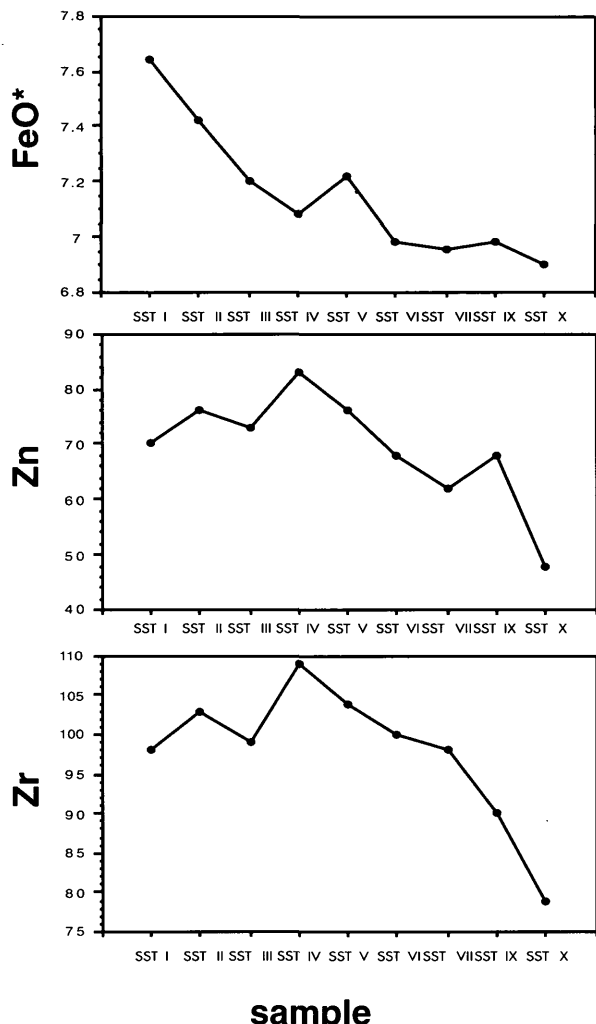
minerals such as baryte and celestite, exclusively occurring in cavities. Comparing table 3 with fig. 7 it is easy to note that the values of these and other trace elements are depleted in samples where these inclusions have been removed. The elements Zn and Zr, normally assumed to be immobile, show slight enrichment. Other elements, Co, Cr, Cu, Ni, Nb, V, and Y do not show significant trends, but scattering values. No depletion of elements due to alteration is observed.

Where dikes are altered due to other fluids, perhaps of non-magmatic origin, cavities with baryte, celestite, laumontite and quartz have never been observed, only small cavities filled with calcite and chlorite are found. Trace elements do not show significant enrichment or depletion.

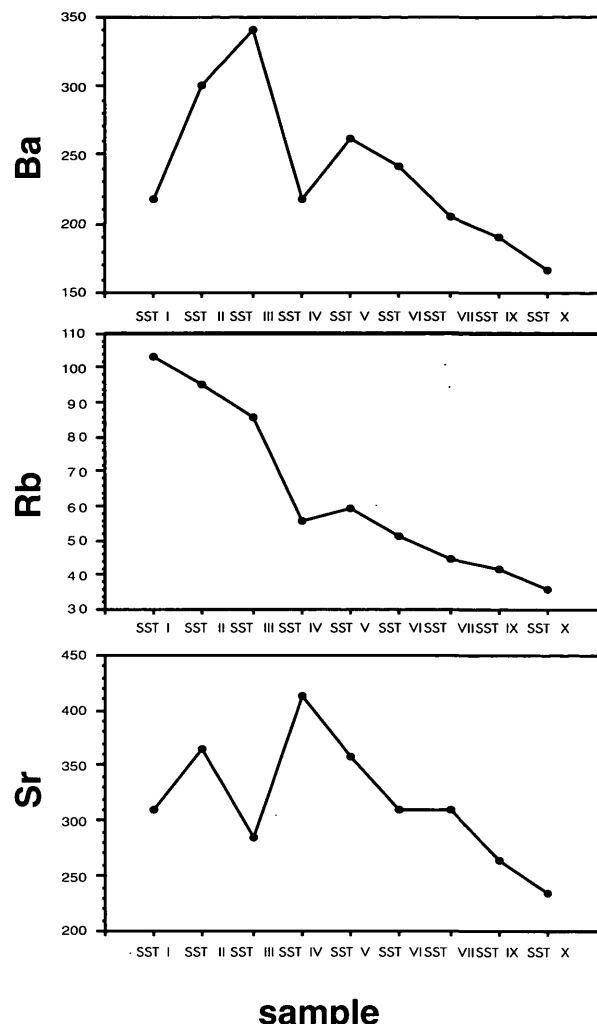
8. Discussion

The basalts are products of an early stage of magma evolution and cannot be considered as primitive parental magma, due to their trace element chemistry and the low MgO and high Al_2O_3 content. According to ULMER et al., 1983, such basalts result from a fractionation of olivine, spinel and Al-poor clinopyroxene in a deep-seated magma chamber. The crystallization of almost pure diopside and anorthite and the absence of biotite and K-feldspar in the basalts suggest Ca-rich primary melt, further depleted in Ti, P, Y, and Zr.

Amphibole xenocrysts and cumulates of amphibole + plagioclase in the andesites indicate a magma evolution dominated by amphibole fractionation. This may be proved by the lack of olivine, because according to KUSHIRO, 1974, plagioclase in presence of amphibole and pyroxene is stable only after the disappearance of olivine. Therefore, we assume two different fractionation processes. While the first, described above, produced the basalts, the second produced the andesites through segregation of amphibole + plagioclase \pm diopside. The fractionation of amphiboles causes depletion of Mg, Fe,



sample



sample

Fig. 7: The postmagmatic alteration is shown by the behavior of FeO* and trace elements, which increase with increasing alteration (decreasing dike thickness = decreasing sample number). The location of the samples is shown in fig. 6. Note that values much lower than the expected trend (especially of the samples SST I – SST III) arise from removing the filled cavities before analysing bulk rock chemistry.

Ca, Al and minor Ti and Y and strong enrichment of Si in the residual melt (CAWTHON, 1976), trends documented by the bulk rock chemistry. The depletion of Al is too slight, in regard to the other elements. The fractionation of Al-free clinopyroxene, which occurs in some cumulates, in the basalts and as xenocrysts in all andesites may be an explanation for this. The occurrence of amphibole- and diopside xenocrysts with corroded rims may document resorption of cumulus material through magma mixing or mingling; perhaps due to convection in a stratified magma chamber as proposed by DAL PIAZ et al.,

1979; LAUBSCHER, 1983; ULMER et al., 1983, for the Adamello.

9. Conclusions

Field evidence indicates that the two-phase dikes originated from successive pulses of evolving magma following the ascent path prepared by the early intrusion. The following magma was emplaced when the foregoing one was still hot and incompletely solidified. This

explains the chilled margins and fluidal structures observed at the contact between the two phases and needs the existence of an evolving magma chamber.

The older magma-pulse emplaced basalts/basaltic andesites, the younger one andesites. Magma evolution through fractionation of amphibole, magnetite, Al-poor clinopyroxene and minor plagioclase in a deep-seated magma chamber is implied by the occurrence of cumulate-xenolithes and xenocrysts of amphiboles and diopsides in the andesites, and by mineral and rock chemistry as well. The observed occurrence of basalts and andesites, generated from the same magmatic source at nearly the same time in a restricted area suggests that the models of chronology, geochemistry and distribution of the periadriatic intrusions proposed by GATTO et al., 1976, and PURTSCHELLER & MOGESSIE, 1988, are too simple.

An estimate of the varying degrees of alteration shows that autohydrothermal, CO₂- and SO₄- bearing fluids slightly enrich the rocks with Zn and Zr, and strongly with Ba, Rb, Sr, until baryte, celestite together with laumontite, calcite and quartz crystallize in the numerous cavities. At the same time phenocrysts and matrix are hydrated and replaced by water-bearing minerals (increasing L.O.I.). Good chemical classification of these rocks is possible after careful sampling and sample preparation (removing of filled cavities) and recalculating all major elements anhydrous to 100%.

10. Acknowledgements

We would like to thank E. Mersdorf and R. Tessadri for their assistance and greatful help during mineral and rock analyses. R. Tessadri and A. Mogessie are thanked for reviewing the draft manuscript, and for critical comments and helpful discussions.

We are greatful to M. Tessadri-Wackerle for reviewing the english version.

11. References

- ALLEGRE, C.J., TREUIL, M., MINSTER, J.F. MINSTER, B. & ALBAREDE, F. (1977): Systematic use of trace elements in igneous processes. Part I: fractional crystallisation process in volcanic suites. – *Contrib. Mineral. Petrol.*, **60**, 57–75.
- ALLEGRE, J.C. & MINSTER, J.F. (1978): Quantitative models of trace element behaviour in magmatic processes. – *Earth Planet. Sci. Lett.*, **38**, 26–43.
- ANDREATTA, C. (1942): Sulle rocce eruttive del Gruppo Ortles-Cevedale. – *Rend. Acc. Italia, cl. Sc. Fis.*, **3**, 298–304.
- ANDREATTA, C. (1951): Carta delle Tre Venezie, Foglio Monte Cevedale. – Magistrato delle Acque, Venezia.
- ANDREATTA, C. (1953): Syntektonische und posttektonische magmatische Erscheinungen der Ortlergruppe in Beziehung zum alpinen Magmatismus. – *TMPM.*, **3**, 93–114.
- BACON, R.C. (1986): Magmatic inclusions in silicic and intermediate volcanic rocks. – *J. Geophys. Res.*, **91**, 6091–6112.
- BECCALUVA, L., GATTO, G., GREGNANIN, A., PICCIRILLO, E. & SCOLARI, A. (1979): Geochemistry and petrology of dyke magmatism in the Alto Adige (Eastern Alps) and its geodynamic implications. – *N. Jb. Geol. Paläont. Mh. Stuttgart*, **6**, 321–339.
- BECCALUVA, L., BIGIOGGERO, B., CHIESA, S., COLOMBO, A., FANTI, G., GATTO, G.O., GREGNANIN, A., MONTRASIO, A., PICCIRILLO, E.M. & TUNESI, A. (1983): Post-collisional dyke magmatism in the Alps. – *Mem. Soc. Geol. It.*, **26**, 341–359.
- BENCE, A.E. & ALBEE, A.L. (1968): Empirical correction factors of the electron microanalysis of silicates and oxides. – *J. Geol.*, **76**, 382–403.
- CALLEGARI, E. (1983): Geological and petrological aspects of the magmatic activity at Adamello (Northern Italy). – *Mem. Soc. Ital.*, **26**, 83–101.
- CAWTHORN, R.G. & BROWN, P.A. (1976): A model for the formation and crystallisation of corundum-normative calc-alkaline magmas through amphibole fractionation. – *J. Geology*, **84**, 467–476.
- CAWTHORN, R.G. & O'HARA, M.J. (1976): Amphibole fractionation in calc-alkaline magma genesis. – *Am. J. Sci.*, **276**, 309–329.
- CONRAD, W.K. & KAY, R.W. (1983): Ultramafic and mafic inclusions from Adak island: crystallisation hi-

- story, and implications for the nature of primary magmas and crustal evolution in the Aleutian arc. – *J. Petrol.*, **25**, 88–125.
- DAL PIAZ, G.V. & VENTURELLI, G. (1983): Brevi riflessioni sul magmatismo post-ofiolitico nel quadro della evoluzione spazio-temporale delle alpi. – *Mem. Soc. Ital.*, **26**, 5–19.
- DAL PIAZ, G. V., DEL MORO, A., MARTIN, S. & VENTURELLI, G. (1988): Post-collisional magmatism in the Ortler-Cevedale massif, Northern Italy. – *Jb. Geol. B.-A.*, **131**, 533–551.
- DIETRICH ,V.J., MERCOLLI, I. & OBERHÄNSLI, R. (1988): Dacite, High-Alumina-Basalte und Andesite als Produkte amphiboldominiierter Differentiation (Aegina und Methana, Ägäischer Inselbogen). – *Schweiz. Mineral. Petrogr. Mitt.*, **68**, 21–39.
- DEL MORO, A., DAL PIAZ, G.V., MARTIN, S., VENTURELLI G. (1981): Dati radiometrici e geochimici preliminari su magmatiti oligoceniche del settore meridionale del Massiccio Ortles-Cevedale. – *Rend. Soc. Geol. It.*, **4**, 265–266.
- DEUTSCH, A. (1984): Young alpine dykes south of the Tauern Window (Austria): a K/Ar and Sr isotope study. – *Contrib. Min. Petrol.*, **85**, 45–57.
- FLOYD, P. A. & WINCHESTER, J. A. (1975): Magma type and tectonic setting discrimination using immobile elements. – *Earth Planet. Sci. Lett.*, **27**, 211–218.
- GATTO, G. O., GREGNANIN, A., PICCIRILLO, E. M. & SCOLARI, A. (1976): The andesitic magmatism in the South-Western Tyrol and its geodynamic significance. – *Geol. Rundschau Stuttgart.*, **65**, 691–700.
- GATTO, G. O., GREGNANIN, A., MOLIN, G. M., PICCIRILLO, E. M. & SCOLARI, A. (1976): Le manifestazioni andesitiche polifasiche dell'Alto Adige occidentale nel quadro geodinamico alpino. – *Studi Trentini Sc. Nat.*, **53**, 21–47.
- GULSON, B. L. (1973): Age relations in the Bergell region of the South-East Swiss Alps, with some geochemical comparisons. – *Eclogae Geol. Helv.*, **66**, 293–313.
- HAMMER, W. (1908): Die Ortlergruppe und der Ciavallatschkamm. – *Jb. Geol. R.-A.*, **58**, 79–196.
- JAKES, P. & WHITE, A. J. R. (1972): Hornblendes from calc-alcaline volcanic rocks of island arcs and continental margins. – *Am. Min.*, **57**, 887–902.
- JAKES, P. & WHITE, A. J. R. (1972): Major and trace element abundances in volcanic rocks of orogenic areas. – *Geol. Soc. Am. Bull.*, **83**, 29–40.
- LAUBSCHER, H. P. (1983): The late alpine (periadriatic) intrusions and the Insubric Line. – *Mem. Soc. Geol. It.*, **26**, 21–30.
- LE BAS, M.J., LE MAITRE, R.W. & WOOLEY, A.R. (1992): The Construction of the Total Alkali-Silica Chemical Classification of Volcanic Rocks. – *Min. Pet.*, **46**, 1–22.
- LE MAITRE R. W. (1984): A proposal by the IUGS sub-commission on the total alcali silica (TAS) diagramm. – *Austral. Journ. Earth Sci.*, **31**, 243–255.
- MOGESSIE, A., TESSADRI, R. & VELTMAN, C. B. (1990): Emp-Amph – a hypercard program to determine the name of an amphibole from electron microprobe analysis according to the International Mineralogical Association Scheme. – *Computers & Geosciences*, **16**, 309–330.
- MÜLLER, D., ROCK, N.M.S. & GROVES, D.I. (1992): Geochemical Discrimination Between Shoshonitic and Potassic Volcanic Rocks in Different Tectonic Settings: a Pilote Study. – *Min. Pet.*, **46**, 259–289.
- MYASHIRO, A. (1973): The troodos ophiolitic complex was probably formed in an island arc. – *Earth Planet. Sci. Lett.*, **19**, 218–224.
- PEARCE, J. A. & CANN, J.R. (1973): Tectonic setting of basic volcanic rocks determined using trace element analyses. – *Earth Planet Sci. Lett.*, **19**, 290–300.
- PEARCE, J. A. & NORRY, M. J. (1979): Petrogenetic implications of Ti, Zr, Y, and Nb variations in volcanic rocks. – *Contrib. Mineral. Petrol.*, **69**, 33–47.
- PECCERILLO, A. & TAYLOR, S. R. (1976): Geochemistry of Eocene calcalcaline volcanic rocks from the Kastamonu area, northern Turkey. – *Contrib. Miner. Petrol.*, **58**, 63–81.
- PURTSCHELLER, F. & RAMMLMAIR, D. (1982): Alpine metamorphism of diabase dikes in the Ötztal-Stubaier Metamorphic Complex. – *TMPM*, **29**, 205–221.
- PURTSCHELLER, F. & MOGESSIE, A. (1988): Dikes from Ortler, Sarntal Alps and Brixen Granite: Mineralogy, Chemical Composition and Petrogenesis. – *Min. Pet.*, **38**, 17–35.
- RAMMLMAIR, D. (1980): Petrographie der Diabase der Ötztaler/Stubaier Masse. – Unveröff. Diss. Univ. Innsbruck, 98 p.
- SMITH, R. E. & SMITH, S. E. (1976): Comments on the use of Ti, Zr, Y, Sr, K, P and Nb in classification of

- basaltic magmas. – *Earth Planet. Sci. Lett.*, **32**, 114–120.
- STACHE, G. (1876): Über die alten andesitischen Eruptivgesteine des Ortlergebietes. – *Verh. k. k. Geol. R.-A.*, **14**, 346–347.
- STACHE, G. & JOHN, C. (1879): Geologische und petrographische Beiträge zur Kenntnis der älteren Eruptiv- und Massengesteine der Mittel- und Ostalpen. II. Das Cevedale-Gebiet als Hauptdistrict älterer dioritischer Porphyrite (Paläoporphyrite). – *Jb. Geol. R.-A.*, **2**, 317–404.
- STACHE, G. (1879): Die Eruptivgesteine des Cevedale-Gebietes. – *Verh. k. k. Geol. R.-A.*, **3**, 66–70.
- THORPE, R. S., VENTURELLI, G., DAL PIAZ, G. V. & POTTS, P. J. (1981): Distribuzione di Terre Rare e di altri elementi in tracce in filoni calccalini ed ultrapotassici oligocenici delle alpi occidentali interne (osservazioni preliminari). – *Rend. Soc. Geol. It.*, **4**, 263–264.
- TOMASI, L. (1950): Studi petrografici dei filoni e contatti del Passo della Bottiglia (Gruppo dell'Ortler). – *Acta Geol. Alpina*, **2**, 1–52.
- ULMER, P., CALLEGARI, E. & SONDEREGGER, U. C. (1983): Genesis of the mafic and ultramafic rocks and their genetical relations to the tonalitic-trondhjemite granitoids of the southern part of the Adamello Batholith, (Northern Italy). – *Mem. Soc. Geol. It.*, **26**, 171–222.
- VENTURELLI, G., THORPE, R. S., DAL PIAZ, G. V., DEL MORO, A. & POTTS, P. J. (1984): Petrogenesis of calc-alkaline shoshonitic and associated ultrapotassic Oligocene volcanic rocks from the Northwestern Alps, Italy. – *Contrib. Min. Petr.*, **86**, 209–292.
- WINCHESTER, J. A. & FLOYD, P. A. (1976): Geochemical discrimination of different magma series and their differentiation products using immobile elements. – *Chem. Geol.*, **20**, 325–343.
- WOOD, D. A., JORON, J. L. & TREUL, M. (1979): A re-appraisal of the use of trace elements to classify and discriminate between magma series erupted in different tectonic settings. – *Earth Planet. Sci. Lett.*, **45**, 326–336.

Authors' address:

Mag. Volkmar Mair, Univ.-Prof. Dr. Fridolin Purtscheller, Institut für Mineralogie und Petrographie, Innrain 52, A-6020 Innsbruck, Austria.

Manuscript submitted: October 5, 1994

Table 1: representative mineral analyses

Table 2: representative bulk rock analyses

Table 3: changes in mineralogy and petrography with increasing alteration.

Table 1: representative mineral analyses, feldspars

sample	cumulate		basalt		basaltic andesite		andesite				
	Bt 20a R	Sf I core	Sf I rim	SF V core	SF V rim	Ep2 a	Ep2 b	Ep2 c	Sf II core	Sf II rim	Sf III core
SiO ₂	44,35	43,92	45,18	46,21	48,39	66,11	62,92	64,48	50,85	47,32	52,28
TiO ₂	0,02	0,03	0,04	0,01	0,03	0,01	0,01	0,01	0,00	0,03	0,03
Al ₂ O ₃	35,68	35,21	34,91	34,47	31,44	22,38	21,68	23,49	31,07	29,04	33,95
FeO	0,35	0,56	0,57	0,36	0,49	0,00	0,07	0,06	0,18	0,21	0,20
MnO	0,00	0,00	0,00	0,00	0,01	0,02	0,01	0,00	0,00	0,03	0,02
MgO	0,11	0,16	0,16	0,16	0,16	0,16	0,15	0,47	0,79	0,09	0,15
CaO	19,55	18,67	17,99	17,11	14,18	2,47	3,72	3,74	13,32	10,76	16,26
Na ₂ O	0,58	0,97	1,47	1,72	3,60	9,78	8,99	6,50	4,27	5,85	2,48
K ₂ O	0,04	0,11	0,14	0,44	0,49	0,08	0,04	0,07	0,14	0,23	0,20
total	100,68	99,63	100,46	98,79	100,00	99,91	99,14	99,92	100,91	100,60	100,26
cations (8 O_x)											
Si	2,041	2,045	2,082	2,119	2,250	2,871	2,786	2,833	2,319	2,450	2,367
Al	1,936	1,932	1,896	1,863	1,723	1,145	1,132	1,216	1,670	1,535	1,627
Fe	0,013	0,022	0,022	0,024	0,019	0,000	0,003	0,002	0,007	0,008	0,007
Mg	0,008	0,011	0,011	0,011	0,011	0,010	0,010	0,052	0,006	0,010	0,007
Ca	0,946	0,931	0,888	0,841	0,706	0,115	0,176	0,176	0,651	0,517	0,796
Na	0,052	0,088	0,131	0,153	0,325	0,823	0,772	0,554	0,378	0,509	0,220
K	0,002	0,007	0,008	0,026	0,029	0,004	0,002	0,004	0,008	0,013	0,012
Ti	0,001	0,001	0,001	0,001	0,001	0,000	0,000	0,000	0,000	0,001	0,001
Mn	0,000	0,000	0,000	0,000	0,001	0,000	0,000	0,000	0,001	0,001	0,001
total	4,999	5,037	5,039	5,037	5,064	4,969	5,034	4,837	5,039	5,043	5,009
albite	5,08	8,54	12,78	15,00	30,62	87,34	81,20	75,47	36,43	48,97	21,39
anorthite	94,69	90,82	86,42	82,47	66,64	12,19	18,57	24,00	62,79	49,77	77,48
orthoclase	0,23	0,64	0,80	2,53	2,74	0,47	0,24	0,54	0,79	1,27	1,14

Table 1: representative mineral analyses, hornblendes

sample	cumulate			basalt			basaltic andesite		
	Bt 20 core	Bt 20 rim	92/18	Sf a core	Sf a center	Sf a rim	Sf d core	Sf d center	Sf d rim
SiO ₂	40,90	41,20	39,41	42,04	41,31	42,00	42,65	41,76	42,02
TiO ₂	1,68	1,66	1,72	1,50	1,75	1,92	1,91	1,69	1,95
Al ₂ O ₃	14,37	14,90	15,19	13,00	13,12	13,17	12,67	13,32	13,53
Cr ₂ O ₃	0,03	0,00	0,01	0,00	0,04	0,02	0,02	0,01	0,05
FeO	13,73	13,05	13,94	12,57	14,41	11,80	12,33	14,43	11,70
MnO	0,14	0,18	0,21	0,19	0,23	0,14	0,22	0,22	0,09
MgO	11,66	12,03	12,42	14,28	12,28	13,56	13,61	12,58	13,91
CaO	11,98	12,09	12,08	11,25	11,78	11,94	12,13	11,82	12,01
K ₂ O	0,92	0,72	0,66	0,48	0,55	0,62	0,56	0,53	0,59
Na ₂ O	1,97	1,98	1,78	1,68	1,79	1,85	1,82	1,90	1,94
total	97,38	97,81	97,42	96,99	97,26	97,04	97,92	97,76	98,42
cations (FM = 13)									
Si	6,039	6,017	5,757	6,039	6,053	6,126	6,167	6,055	6,066
Al ^{IV}	1,961	1,983	2,243	1,961	1,947	1,874	1,833	1,945	1,934
Al ^{VI}	0,540	0,577	0,373	0,239	0,314	0,387	0,330	0,329	0,366
Fe ³⁺	0,506	0,564	1,092	1,389	0,940	0,674	0,726	0,932	0,766
Ti	0,186	0,184	0,193	0,164	0,194	0,210	0,209	0,183	0,208
Cr	0,000	0,000	0,000	0,000	0,009	0,000	0,000	0,009	0,000
Mg ₂₊	2,563	2,613	2,704	3,054	2,683	2,944	2,936	2,718	2,994
Fe ₂₊	1,188	1,032	0,611	0,121	0,829	0,763	0,769	0,818	0,649
Mn	0,018	0,026	0,026	0,026	0,018	0,026	0,026	0,026	0,017
Ca	1,898	1,895	1,887	1,734	1,847	1,867	1,876	1,838	1,857
K	0,177	0,132	0,123	0,086	0,106	0,114	0,104	0,096	0,113
Na	0,568	0,561	0,500	0,466	0,510	0,526	0,513	0,531	0,547
total	15,644	15,584	15,509	15,458	15,512	15,489	15,471	15,518	15,441

Table 1: representative mineral analyses, hornblendes and pyroxenes

sample	andesite			cumulate			basalt			basaltic andesite			andesite		
	Bt 5 core	Bt 5 center	Bt 5 rim	Bt 3 core	Bt 3 rim	sample	92/20 Px	Ep2 Px 3	Ep2 Px 1	Ep2 Px 2	ESA 1 Px	ESA 2 Px 1	ESA 2 Px 2	ESA 1 Px	
SiO ₂	43,89	41,91	42,45	43,77	41,04	SiO ₂	46,81	47,98	50,54	50,09	51,39	52,42			
TiO ₂	1,65	1,57	1,57	1,49	1,51	TiO ₂	0,79	0,71	0,60	0,68	0,34	0,14			
Al ₂ O ₃	12,15	13,49	13,30	12,39	14,45	Al ₂ O ₃	7,78	5,51	4,39	3,85	3,49	2,32			
Cr ₂ O ₃	0,01	0,00	0,00	0,02	0,00	Fe ₂ O ₃ *	5,15	6,50	0,00	3,91	2,23	2,09			
FeO	12,15	15,07	14,84	10,57	15,94	FeO *	3,65	1,77	9,28	5,58	2,80	1,81			
MnO	0,18	0,30	0,33	0,17	0,31	MnO	0,14	0,13	0,28	0,26	0,14	0,07			
MgO	14,25	11,77	11,78	15,02	10,67	MgO	13,45	14,63	12,70	14,49	15,60	17,10			
CaO	10,63	10,67	10,66	10,69	10,53	CaO	21,46	22,45	21,83	21,75	23,33	23,04			
K ₂ O	0,51	0,54	0,49	0,46	0,51	K ₂ O	0,04	0,02	0,03	0,03	0,03	0,03			
Na ₂ O	1,92	1,97	1,83	1,94	1,90	Na ₂ O	0,28	0,26	0,11	0,19	0,22	0,18			
total	97,34	97,29	97,25	96,52	96,86	total	99,55	99,96	99,76	100,83	99,57	99,20			
cations (FM = 13)															
Si	6,263	6,074	6,156	6,259	6,017	Si	1,745	1,779	1,893	1,851	1,893	1,924			
Al IV	1,737	1,926	1,844	1,741	1,983	Al 3+	0,342	0,241	0,194	0,168	0,151	0,100			
Al VI	0,305	0,414	0,432	0,348	0,510	Fe 3+	0,145	0,181	0,000	0,109	0,062	0,058			
Fe 3+	1,190	1,223	1,146	1,154	1,188	Fe 2+	0,114	0,055	0,291	0,172	0,086	0,056			
Ti	0,180	0,174	0,174	0,163	0,167	Mg	0,747	0,809	0,709	0,798	0,856	0,936			
Cr	0,000	0,000	0,000	0,000	0,000	Ca	0,857	0,892	0,876	0,861	0,921	0,906			
Mg	3,038	2,541	2,546	3,207	2,334	Na	0,020	0,019	0,008	0,014	0,016	0,013			
Fe 2+	0,260	0,605	0,659	0,110	0,767	K	0,002	0,001	0,001	0,001	0,001	0,001			
Mn	0,026	0,035	0,044	0,017	0,035	Ti	0,022	0,020	0,017	0,019	0,009	0,004			
Ca	1,630	1,653	1,657	1,642	1,656	Mn	0,004	0,004	0,008	0,004	0,004	0,002			
K	0,094	0,096	0,087	0,086	0,097	total	3,998	4,001	3,998	4,001	3,999	4,000			
Na	0,532	0,557	0,514	0,542	0,537	enstatite	43,50	46,07	37,80	43,58	45,96	49,32			
total	15,255	15,298	15,259	15,269	15,291	ferrosilite	6,62	3,13	15,50	9,41	4,63	2,93			
						wollastonite	49,88	50,81	46,70	47,01	49,40	47,76			
cations (6 O _x)															

Table 2: representative bulk rock analyses (Fe_{tot} as Fe₂O₃)

		inclusions						basaltic andesites, andesites					
Probe	Bt 20	Ep 4 f	SST I	SST II	SST III	SST IV	SST V	SST VI	SST VII	SST VIII	SST IX	SST X	LF
SiO ₂	42,99	52,75	53,10	54,57	57,27	57,80	56,19	55,67	55,40	56,79	56,83	56,17	54,91
TiO ₂	1,41	0,76	0,69	0,70	0,66	0,67	0,61	0,62	0,67	0,62	0,66	0,64	0,60
Al ₂ O ₃	16,87	17,14	17,69	18,53	16,97	17,04	6,94	17,76	6,70	6,82	6,52	6,77	16,74
Fe ₂ O ₃	12,11	8,98	0,20	0,16	0,15	0,16	0,14	0,13	0,18	0,13	0,15	0,15	7,04
MnO	0,15	3,69	3,17	2,93	3,02	3,06	2,94	3,04	3,17	2,72	2,95	2,92	0,12
MgO	12,81	7,10	5,84	6,71	5,92	5,98	6,02	7,83	7,40	7,76	7,59	7,59	3,10
CaO	1,35	2,74	3,04	3,01	2,31	3,97	4,31	3,65	3,41	2,85	3,07	3,07	7,12
Na ₂ O	0,83	2,29	1,41	2,02	1,49	1,21	1,59	1,49	1,56	1,62	1,34	1,34	3,57
K ₂ O	0,06	0,16	0,17	0,17	0,18	0,18	0,19	0,17	0,22	0,21	0,21	0,20	1,30
P ₂ O ₅	0,06	0,02	0,04	0,07	0,08	0,04	0,13	0,05	0,07	0,19	0,19	0,17	0,17
SO ₃	0,06	4,66	7,44	5,10	3,88	2,04	2,23	3,95	2,02	2,34	2,48	0,06	0,09
L.O.I.	2,19	99,49	99,82	100,13	99,65	99,89	100,06	99,29	99,35	99,54	100,22	99,83	99,97
Total	99,79												
trace elements (ppm)													
Ba	60	308	217	300	341	218	261	241	205	208	190	166	268
Co	68	22	<5	<5	<5	6	<5	<5	<5	<5	7	<5	5
Cu	12	10	12	12	12	10	12	15	6	23	16	11	13
Ni	54	<5	20	20	<5	19	18	<5	<5	<5	8	5	28
Pb	35	10	<5	<5	<5	<5	<5	<5	<5	<5	7	10	<5
Rb	9	6	10	10	<5	7	<5	<5	<5	<5	5	5	<5
Sr	<5	72	103	95	86	56	59	51	45	50	42	36	31
V	19	279	310	366	285	412	359	311	310	271	264	235	247
Y	225	133	130	127	143	137	135	144	113	122	114	114	144
Zn	22	16	17	18	18	20	19	19	19	17	15	15	14
Zr	70	67	70	76	73	83	76	68	62	99	68	48	52
	31	65	98	103	99	109	104	100	98	93	93	90	72

Table 2: representative bulk rock analyses (Fe^{tot} as Fe₂O₃)

Probe	basaltic andesites, andesites										basalts													
	Bt 2	Bt 3	Bt 5	Ed 5	Ed 3	Ep 1	Ep 4 g	Sf III	Ed 3	Ed 4	Ep 2	Sf I	Sf V	Ba	Co	Cr	Cu ⁰	Ni ⁰	Pb	Rb	Sr	V	Y	Zn
SiO ₂	57,62	56,02	56,53	57,97	57,48	54,25	59,69	53,98	50,49	49,50	50,88	49,23	48,66											
TiO ₂	0,64	0,60	0,62	0,59	0,58	0,49	0,58	0,65	0,78	0,81	0,83	0,86	0,86											
Al ₂ O ₃	18,11	17,46	17,49	16,31	17,31	16,54	16,33	17,11	16,61	16,31	16,95	17,35	17,81											
Fe ₂ O ₃	6,78	6,73	6,72	7,04	7,23	0,17	0,15	6,59	7,48	9,06	9,56	9,51	9,61											
MnO	0,15	0,10	0,16	0,17	0,17	2,99	2,79	0,18	0,13	0,18	0,18	0,14	0,15											
MgO	3,05	2,95	2,95	2,99	2,99	2,78	3,98	3,04	3,85	4,17	3,72	4,52	5,26											
CaO	7,27	7,55	7,46	4,71	6,78	6,96	6,14	6,52	7,11	7,94	8,20	9,41	8,51											
Na ₂ O	2,95	2,78	3,07	4,50	2,76	2,90	2,90	3,84	3,19	1,98	3,00	2,54	3,22											
K ₂ O	1,71	1,50	1,58	1,83	2,48	1,72	1,78	0,98	1,07	1,77	0,79	0,49	0,63											
P ₂ O ₅	0,18	0,19	0,22	0,14	0,21	0,19	0,20	0,13	0,14	0,17	0,20	0,12	0,15											
SO ₃	0,05	0,08	0,11	0,01	0,01	0,14	0,07	0,01	0,05	0,17	0,59	0,15	0,06											
L.O.I.	2,00	4,19	2,79	3,54	2,07	5,68	5,68	2,71	5,08	6,54	7,93	4,13	4,94	4,72										
total	100,51	100,15	99,70	99,80	100,00	100,25	100,15	99,80	99,51	99,79	99,46	99,97	99,89											
trace elements (ppm)																								
Ba	255	200	225	337	417	521	315,00	193	161	161	92	145	113											
Co	9	<5	6	7	<5	6	<5	<5	7	7	18	13	148											
Cr	15	14	15	21	24	16	23	6	24	19	17	16	31											
Cu ⁰	23	18	21	8	<5	<5	<5	<5	11	44	44	25	32											
Ni ⁰	<5	<5	10	<5	<5	10	<5	<5	8	17	17	13	22											
<5	5	<5	5	5	<5	5	<5	<5	11	<5	10	10	13											
<5	43	41	51	53	109	51	72	33	40	6	<5	<5	<5											
339	276	312	162	294	251	124	138	135	284	287	248	195	242											
143	136	162	20	151	17	17	17	16	194	253	243	243	228											
21	86	87	83	91	109	68	76	99	54	58	70	72	89											
120									89	88	69	65	67											

← increasing alteration ← decreasing dike thickness

sample	SST I	SST II	SST III	SST IV	SST V	SST VI	SST VII	SST IX	SST X
dike thickness	0.3 m	0.5 m	0.8 m	1 m	1.5 m	2 m	dike sharing	3 m	3 bis 4 m
color	dark green-black	dark green-black	dark grey	grey	light grey	light grey reddish	light grey	light grey	light grey
texture	massive filled cavities with quartz, calcite, baryte, celestite, laumontite	massive filled cavities with quartz, calcite, baryte, celestite	fine-grained only few filled cavities	porphyritic filled cavities with quartz, calcite	porphyritic	porphyritic	porphyritic	porphyritic	porphyritic
thin section	the few fsp and hbl phenocrysts in the glassy matrix are pseudomorphically replaced by cc, chl, ep and mt. The zoning of the primary minerals is preserved by zoning of the various amounts of secondary minerals.	the few fsp and hbl phenocrysts in the glassy matrix are pseudomorphically replaced by cc, chl, ep and mt. The hbl are corroded with dark brown rims. The fsp are sericitized and partly replaced by calcite. Some assimilated material of surrounding quartzphyllite.	all hbl are well preserved, while the fsp are totally replaced by sercite and cc. Lots of small cavities filled with cc, quartz, and baryte (see negative value in fig. 7).	the matrix is characterized by light and dark areas (different degrees of alteration). Hbl are well preserved, fsp are totally replaced by sercite and calcite; small cavities filled with chl and laumontite.	the portion of matrix to phenocrysts decreases. Few, but well preserved hbl, all fsp sericitized.	Hbl zoned and well preserved, fsp zoned but slightly sericitized. Matrix unaltered.			

Table 3: changes of petrography and mineralogy with increasing alteration

cc = calcite; chl = chlorite; ep = epidote; fsp = feldspar; hbl = hornblende; mt = magnetite.